

Jan CZERWIŃSKI 
Andreas MAYER
Jörg MAYER
Heinz BURTSCHER 
Thomas LUTZ 
Rainer MAYER
Barbara ROTHEN-RUTISHAUSER 
Joachim FREY
Christian LÄMMLER
Tobias RÜGGERBERG 
Patrick SPECHT

Minimizing indoor infection risks with automotive nanofiltration and with laminar vertical flow

ARTICLE INFO

Received: 7 April 2023
Revised: 12 May 2023
Accepted: 12 June 2023
Available online: 3 July 2023

The knowledge about nanoaerosols, their potential health effects, their measurement, limitation and administrative-legal treatment has been developed in the last 3 decades in connection with the exhaust gas cleaning of the combustion engines. Nanofiltration, which has thus become known, almost completely eliminates nanoparticles with filters of high durability, high specific filtration areas, and reasonable costs. On the occasion of the Covid pandemic, NanoCleanAir experimentally proved that the viruses in an automotive filter substrate are separated as well as the combustion particles and are also deactivated. To minimize cross exchange of infectious aerosol, new attention must be paid to flow management in ventilated spaces. Digitized flow analysis has also received significant inspiration from engine technology in the past. This paper provides information on some basic investigations and gives valuable advice based on the experimental and numerical results of a retrofitted classroom.

Key words: ventilation for virus protection, vertical laminar flow, nanoparticle separation, virus deactivation, ceramic honeycomb wall flow filter, nanofiltration

This is an open access article under the CC BY license (<http://creativecommons.org/licenses/by/4.0/>)

1. General

A SARS CoV-2 infected person may emit up to 10 million viruses with each m³ of exhaled air, and on the other hand, the infection dose may be as low as 500–1000 viruses. Given these numbers, the infection risk in a room cannot be sufficiently reduced by periodic window ventilation or by partly cleaning with mobile air cleaners but requires a continuous perfect virus elimination. Furthermore, lateral flow from the infected persons to their direct or distant neighbors must be avoided. This sounds utopic but can indeed be solved by body heat-induced vertical laminar flow and ventilation from floor to the ceiling, extracting the contaminated air at the ceiling and recycling it via a filter back to the floor. Filtration must be very close to 100%. Since the «naket» Corona virus has a size of 60–150 nm, which is the typical size of particles emitted by combustion engines. The diesel particle filter DPF, a honeycomb type ceramic wall-flow filter, was selected for this nanofiltration task. These filters reach > 99% efficiency for soot particles of 10–500 nm and have attractive properties since their filtration surface is > 1 m² per liter bulk volume, they can easily be cleaned in situ, if needed thermically disinfected or catalytically coated, and have the life, the quality, low bulk and low cost of an automotive product. To test the bioaerosol filtration properties, bacteriophages MS2, which are non-pathogenic to human, animals and plants and have a viral particle size of 30–40 nm were used for the test as a proxy for SARS-CoV-2 virus. The wall flow filters reached a filtration rate of > 99% for these bacteriophages and the survival test resulted in 1% active viruses after 24

hours, zero after 48 hours. To test the whole system, a classroom was selected as a pilot case. The ventilation was designed to exchange the room's air volume five times per hour. Contaminated air was extracted at the ceiling and recycled to the floor corners after filtration. Fresh air from outside supplied for CO₂-control was also filtered to clean it from ultrafine traffic related carcinogenic particles. The dynamic cleaning process and room distribution was tested with salt nanoparticles simulating the virus source by a cloud concentration of 80,000 particles per cubic centimeter. The lateral flow reaching the neighbor desk of the infected schoolboy contained only 2–300 P/cc, demonstrating that the contaminated air escapes vertically, showing a cross-contamination risk reduction of 2–3 orders of magnitude. This virus protection system is universally applicable, not only for applications in classrooms, but can also be scaled and adapted to industry, hospitals and public transport environments including aircraft cabins.

2. Introduction

Corona viruses, like combustion soot, are among the smallest suspended particles [11, 17, 23]. When exhaled by an infected host, they are usually surrounded by a liquid envelope and reach 500–10,000 nm, but the aqueous envelope evaporates rapidly [8], leaving particles with a thin mucus envelope in the size range of 300–500 nm [9, 20]. Once released as an aerosol in indoor air, they remain suspended for many hours. When they reach surfaces that do not contain host cells, they remain firmly bound there by van der Waals forces, like other fine particles, and lose their

activity after a few hours [4]. Today, it is recognized that only consistent suppression of aerosol transmission in closed rooms, where long periods of residence prevail, can reduce the risk of infection [25, 36]. Thus, ventilation is required.

It is further essential to recognize that the air exhaled by an infected person may contain up to 10 million viruses per m³ [10, 27]. In contrast, the infectious dose is only 500–1000 viruses, and that infection can occur with a few minutes' exposure [18]. Thus, it makes little sense to aim for dilution by a factor of 2–5 and be satisfied with filter removal efficiencies of 60–80%, which is often considered sufficient for ventilation. Still, much more efficient methods must be sought to ensure adequate protection.

Firstly, the separation efficiency must be high, especially in the diffusion range, i.e., below 1000 nm. Secondly, the ventilation air flow pattern must under no circumstances lead to lateral transport of the virus cloud, which otherwise would favor cross-contamination and accelerate its spread in the course of turbulent dilution of this cloud. Instead, laminar displacement principles are required that reduce cross-contamination by at least two orders of magnitude, and filtration should reach values > 99.9% in the size range < 1000 nm.

Thus periodic window ventilation seems not very suitable because it tolerates a high concentration towards the end of this period, which can be sufficient for contagion and contributes to the rapid expansion of contamination. Also, the use of portable air cleaners by filtration or UV-light, which clean only part of the air but otherwise mix the air in the room by its turbulent flow pattern contribute strongly to the distribution. [7, 21].

If filtration is used, the air supplied from outside should also be filtered efficiently because urban air contains, among others, cancerogenic ultrafine particles from traffic (soot particles and metal oxide particles from exhaust gas, brake abrasion, tire, and road abrasion) in the same size range as the viruses [30, 35] and in much higher concentrations, namely often > 20,000 particles per cubic centimeter, i.e., about one million more than the maximum expected virus concentration.

Both tasks can be solved in combination, which would finally make a significant contribution to mitigating the high mortality risk [12, 34] from traffic-related nanoparticles and avoiding virus infections. In the following, a new technical approach for a sustainable solution to these tasks is presented, which has already been investigated in a classroom as a pilot application by numerical flow simulation and experimentally by salt particle tracing and has fulfilled the requirements mentioned above during a full year of flawless operation [26, 28].

3. Recent developments of ceramic multicell wall flow filters

Over the past thirty years, a filter development has taken place, which, surprisingly, has been completely limited to the application in the exhaust gas of internal combustion engines. From the beginning, the requirements were very high because of the high temperatures in the exhaust tract, the mechanical and thermomechanical demands, the necessity to manage with a very small bulk volume under vehicle

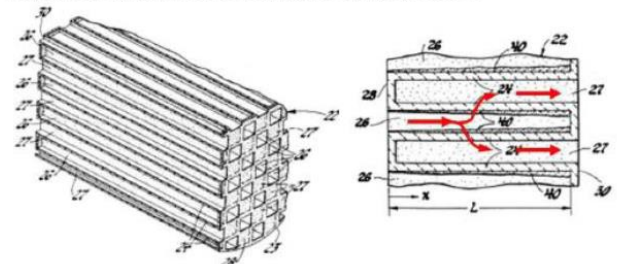
floors at low backpressure, and after the introduction of the particle number criterion by Switzerland with a request for high separation efficiency according to VERT [33] of > 98% for particle sizes from 10 nm. 2007 this has been adopted with slight modifications (lower limit 23 nm) by the EU, later by China, India, and many other countries.

Meanwhile, these filters are used in almost all new vehicles, diesel, petrol, and gas. It is estimated that about 300 million vehicles are equipped with particle filters, i.e., a large series product manufactured at comparatively low cost and subject to the stringent quality criteria of the automotive industry. The author team has been involved in developing this technology and the particle metrology required for it from the beginning [2, 5, 19].

In the course of development, the ceramic wall-flow filter design has emerged as the standard solution [13]. Derived from the multicellular structure of a catalyst substrate, but with porous walls (pore size around 10 μm), flow through the walls is forced by alternately plugging the cells (Fig. 1). Since the sum of the wall areas is very large (up to 1.5 m² per liter of filter volume), the flow velocity is reduced from an inflow around 50 m/s to a flow of about 5 cm/s through the walls. Thanks to this low velocity, the separation of nanoparticles by diffusion in the pore labyrinth is enabled (Fig. 2), and the pressure drop remains within narrow limits set by the engine.

Historical Perspective (Ceramic Wall-Flow Monolith 1979)

Inventors: **Outland; Robert J.** (Grosse Pointe Woods, MI) Assignee: **General Motors Corporation** (Detroit, MI) Appl. No.: 099935 Filed: December 3, 1979. Issued: June 30, 1981, 4,276,071.



Deep-Bed and Surface (cake) Filtration

Fig. 1. Ceramic wall flow filter for Diesel application DPF and gasoline application GPF

Starting in the 80's with a cell density of 100 cells per square inch [cps], today we are at 300 cps and have achieved unprecedented compactness of these filter cells, which allows them to be installed even in small vehicles.

In Diesel engines this filter achieves these high collection efficiencies only after establishing an initial soot layer on the porous filter walls (Fig. 3), which precedes the wall pores with a finer pore structure. This effect of pore gradation can also be achieved by ceramic membrane formation or using hierarchic pore structuring techniques [3] so that filter substrates are available today which reach the high efficiency right from the start and are therefore also suitable for the filtration of viruses, whose concentration in the air is much lower than the concentration of soot particles in the diesel exhaust gas and which would therefore only form a filtering layer after far too long a time.

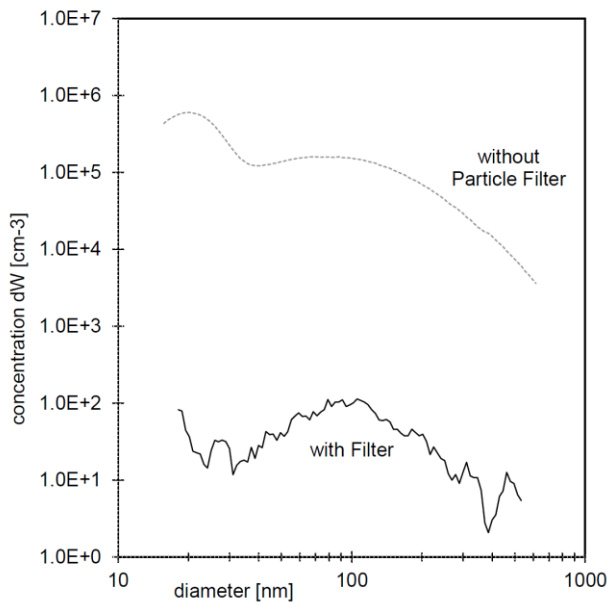


Fig. 2. Diesel soot particle filtration by number > 99% acc. to VERT [33]

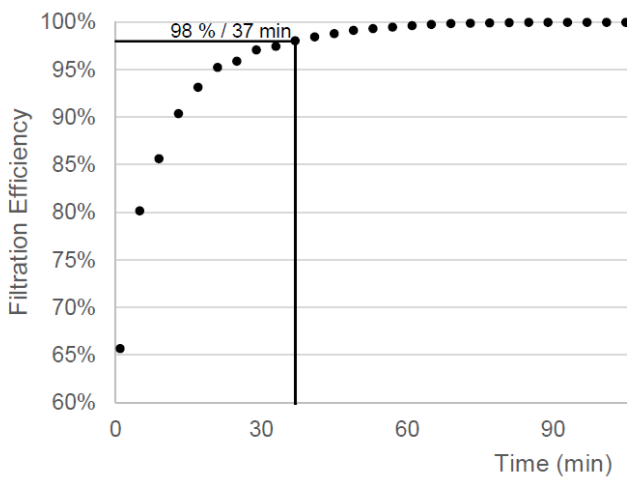


Fig. 3. Filtration efficiency increase by initial soot layer build up on a Diesel engine [33]

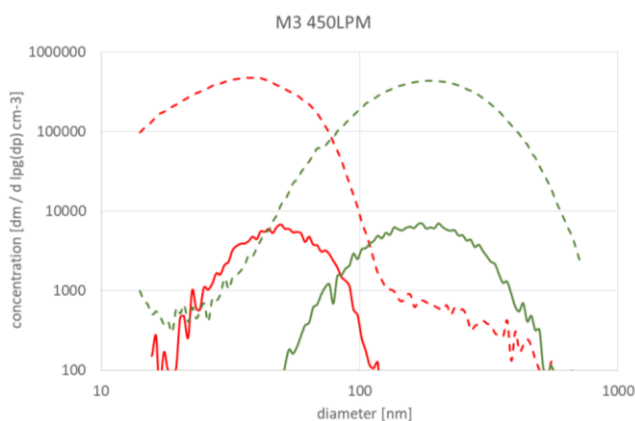


Fig. 4. Filtration of soot generated by two CAST settings [15], measured by SMPS und CNC [31]

These filters have numerous properties which make them suitable for use in exhaust air purification, air condi-

tioning, and, in the present case, for the efficient purification of air from bioaerosols, not only in building services but also in the medical sector and in public transport: low construction volume, light, catalytically coatable, safely heatable for disinfection, easy to clean in situ, do not change their properties due to vibration or wetting or aging and can be easily integrated into a wide variety of geometries and systems.

4. Filtration of infectious bioaerosols

According to the laws of aerosol physics, it may be assumed that viruses behave similarly to soot particles in a filter matrix, i.e. that their flow pattern is determined primarily by mobility, i.e., by size. However, this has to be verified. Therefore, a sensitive test method is needed that provides information on the volumetric concentration of the bioaerosols, and even more precisely, it must provide information on the number of active viruses in the sample volume because the number of deactivated viruses or virus fragments does not make sense for the evaluation of a virus protection filter.

Working with pathogenic viruses, especially highly transmissible ones, poses great health challenges. Due to the high contagiousness (transmissibility) and virulence of SARS viruses in general and SARS-CoV-2 in particular, experiments would have to be carried out under the highest biosafety measures (BSL-3), which makes an experimental facility with aerosols practically impossible.

For these reasons, using bacteriophages as surrogate viruses is state of the art in environmental biology [1, 6, 14, 24, 29]. Bacteriophage MS2 is morphologically, structurally, and genetically similar to human viruses such as SARS-CoV-2, noroviruses, or rotaviruses enabling it to be used as tractable and safe surrogates for human viruses. As a practical surrogate virus, the *Escherichia coli* bacteriophage MS2 can be used together with biological safety laboratory strains of *Escherichia coli* as target cells which are safe for humans and the environment.

MS2 is one of the smallest viruses with a diameter about 2–4 times smaller than SARS-CoV-2. Like SARS-CoV-2, MS2 is a positive-strand RNA bacteriophage. It specifically infects *Escherichia coli* F+ bacteria and can therefore be detected actively (alive) with very high sensitivity in the form of "plaques", which are formed by the multiplication of the viruses in the infected bacterium (up to 1 million viruses in one bacterium) and thus enlarge it to the point where it can be counted visually. In addition, bacteriophage MS2 is highly persistent in aerosols, making it an ideal virus for testing the efficiency of air and water filtration systems; bacteriophage MS2 (ATCC 15597-B1) and its corresponding *Escherichia coli* F+ safety strain C300 (ATCC 15597) are available from the American Type Culture Collection (ATCC).

The following figures show the wind tunnel-like test facility (Fig. 5, 6), sample collection through gelatine filters (Fig. 7), and sample counting the plaques before and after filters (Fig. 8). The equipment and the procedure are described in detail in [28]. Example of result is given in Fig. 9, which illustrates a calculated filtration of > 99.99%.

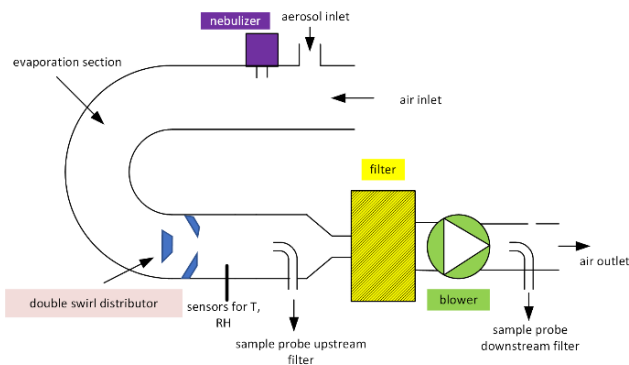


Fig. 5. Flow channel to dry and homogenize salt particles or CAST soot for filter test



Fig. 6. Actual test installation at FHNW with aerosol sampling points for particle counting

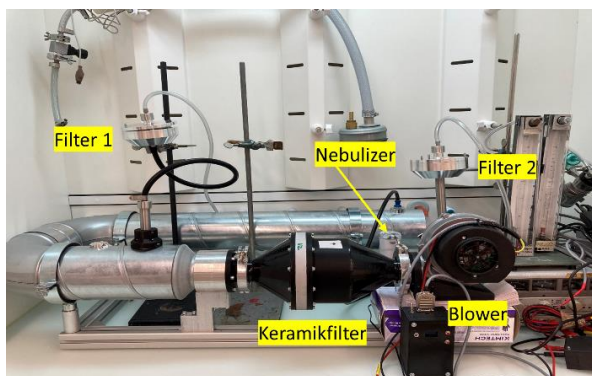


Fig. 7. Test installation at AMI Uni Fribourg for bacteriophage filtration test under the hood



Fig. 8. Agar plates, from which the number of plaques is counted before (left) and after filter (right). The solution was highly diluted to make it countable. Each plaque stays for one original virus

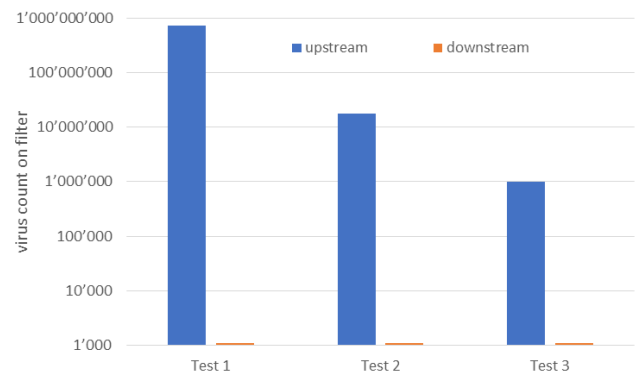


Fig. 9. Typical counting results of « plaques » resulting numerically to values > 99.99%

5. Deactivation of separated viruses in the filter matrix

Filtering alone is not enough because even if the degree of separation is very high, the viruses must be completely deactivated in as short a time as possible, because otherwise there remains an uncertainty as to when, in the course of time, with higher loads or in conjunction with moisture, discharge occurs, so that, as is known with bacteria, the filters themselves could become a dangerous source of pathogenic germs.

In principle, there are many possibilities for disinfection of this type of filter. For example, the filters could be coated with silver or copper or other virucidal substances, or they could be periodically heated to a temperature sufficient for complete disinfection. When used against bacteria, this would certainly be necessary and is basically also provided for this filter design. With viruses, however, the problem may be easier to solve, since viruses are not viable over a long period of time without host cells, they lose their activity or virulence. A detailed report on the loss of activity of SARS CoV-2 viruses deposited on dry solid surfaces is available in [32]. A relatively consistent logarithmic law is shown, although it depends on the materials. After 2–3 days, virulence is hardly detectable. Whether this also applies to the filter materials investigated here had also of course, to be systematically proven.

Paper [28] describes the test shown in Fig. 7: a certain volume of air with a very high concentration of viruses was passed from the test channel in parallel over several small filter samples and analyzed after different times: immediately, after 24 hours, and after 48 hours. Of the 20 million PFU (plaques forming units) that could be counted in the fresh sample, an average of 1–2% were still active after 24 hours at room temperature, and practically none after 48 hours.

Therefore, it can be concluded that, in line with literature, the viruses deposited on the ceramic surfaces rapidly lose their activity even without virucidal coating, i.e., that no active viruses can be discharged. This test should be carried out on all materials used for filtration, and a possible influence of moisture should also be checked.

6. Ventilation to avoid cross contamination in a classroom

It cannot be known who in a group is already infected and can spread the virus through his exhaled air wherever

he goes. Is there a way to avoid infecting people within a distance of 1 m?

Basically there is only one safe place: in the airspace above the heads. This is where the viral cloud must be transported to as soon as possible after exhalation. First and foremost, only body heat can serve this purpose. Every person constantly emits about 100 watts to the environment. Thanks to this heat, a convective movement towards the ceiling takes place in the undisturbed air, which is superimposed by the exhalation speed and slowed down somewhat by the evaporation of moisture (Fig. 10 and 11).

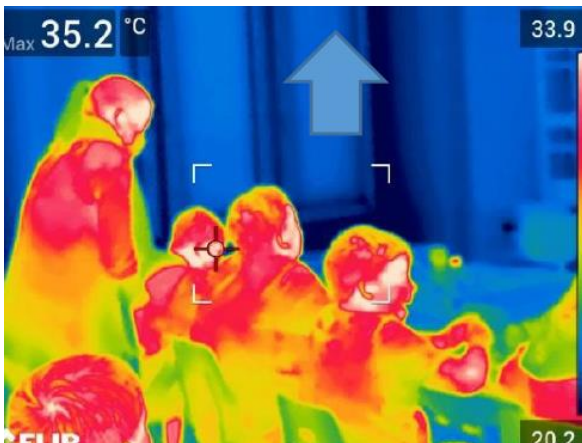


Fig. 10. Infrared camera picture shows the body heat



Fig. 11. Porous textile tubes at the ceiling collect the particles



Fig. 12. Clean air returns to the classroom at the bottom

There is probably only this possibility to quickly remove the viruses from the infection space, and this movement must not be disturbed by turbulence. It must be supported by a laminar displacement of the room air from the bottom to the top.

At the ceiling, the air is extracted without leaving dead-water zones before it would return down along cold walls or windows, then perfectly cleaned in the nanofilter, enriched with fresh air, and returned well-distributed at floor level via skirting boards (Fig. 12). Probably only this approach, derived from the principle of displacement ventilation, can avoid contagion in closed rooms. Even with this method, extreme cases such as coughing and sneezing cannot be controlled, but these will be exceptions that can be controlled by hygienic behavior.

It is clear that this method of transporting the contaminated air by displacement in conjunction with thermal upward drift from the source to the ceiling, where it is collected and extracted, can only serve its purpose if the separation in the filter is very close to 100% because otherwise a part of the viral load would be constantly returned to the room and widely distributed there.

7. The classroom pilot application

The experimental installation shown here does not yet have the character of a finished product but was set up as a laboratory, so to speak, to check the effect of the measures and to carry out an initial optimization. The two figures below (Fig. 13 and Fig. 14) show the room and the installation scheme. The recirculation system is designed for fivefold air exchange per hour and contains a fresh air supply with which the CO₂ level in the fully occupied classroom can be controlled to a setpoint value of around 1200 ppm, i.e., one does not have to accept the large fluctuations of window ventilation. Heat exchange of fresh air and exhaust air supplement the energy balance. The system is deliberately designed to optimize a single room, is compact, and manages with a very low ventilation power.

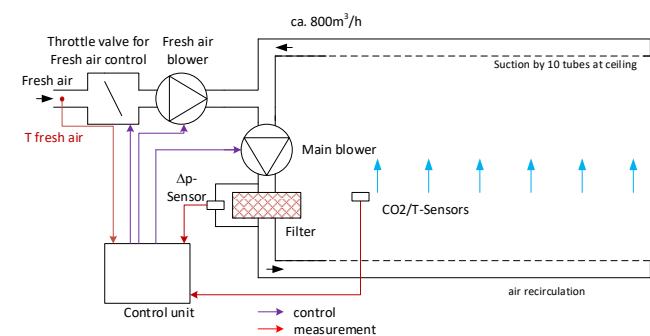


Fig. 13. General arrangement for laminar vertical flow, high nanofiltration, controlled supply of filtered fresh air

The air guidance in textile hoses with well-characterized porosity allows optimum distribution with low turbulence excitation. However, it will still have to be optimized for commercial application, using similar design solutions to those used for displacement ventilation. The principle of avoiding the risk of lateral cross-contamination by capturing emitted viruses overhead and efficiently removing them by nanofiltration can be transferred to many other applica-

tions, especially to applications in the hospital sector and in modes of transport up to aircraft cabins, where the reverse flow direction from top to bottom massively increases the risk of infection today.



Fig. 14. Pilot classroom with hot plates to replace the students body heat

8. Computational flow simulation

Using the SIEMENS STAR-CCM+ software, the schoolroom was digitally simulated to calculate the flow conditions in the entire room in short time steps (Fig. 15). The aim was to represent the three-dimensional flow parameters such as direction and speed in the whole room as a function of the free design parameters such as air exchange rate, flow distribution during suction, backflow as a function of the permeability design of the porous pipes, body temperature, exhaling temperature, filtration efficiency, wall temperature and radiator temperature in their temporal development.

The particles are assumed to be solid particles without post-evaporation using a Lagrangian approach similar to fuel injection in a diesel engine. A two way coupling as an interaction between the particles and the flow and vice versa is used. The 10 students and the teacher realistically exhale and inhale (8 times per minute) and emit 3045 particles per second, which perfectly follow the airflow due to their small size of 100 nm. A particle loss by inhalation is not assumed. Each particle path is tracked and thereby any risk of infection can be detected by marking the particles.

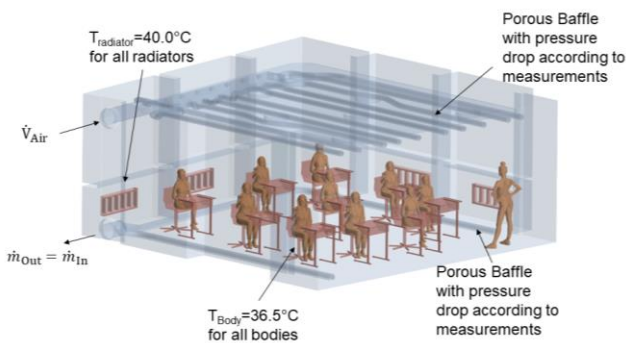


Fig. 15. Digital modelling of the classroom with students and teacher; in the arrangement shown here the flow comes from top to investigate the worst case for virus protection

In the two following illustrations, Fig 16 and Fig 17, it is assumed that the students exhale continuously, and the streamlines starting at the student’s mouth and ending at the porous tubes on the ceiling are computed.

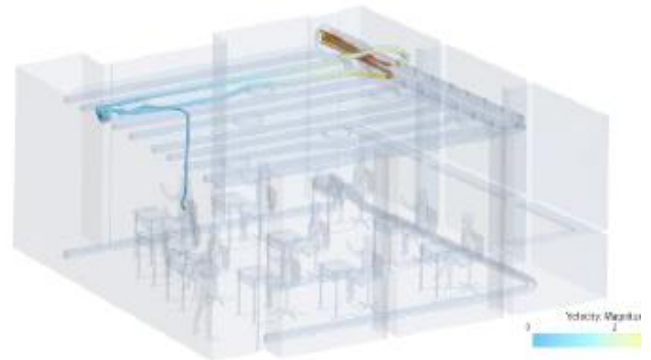


Fig. 16. Ventilation flow from floor to ceiling. Particles are perfectly guided from the infected student to the safe room overhead

This representation is possible for each individual student and also collectively, but then becomes confusing. The protective vertical movement is apparent in all cases, although the current threads form sometimes some unforeseen recirculation zones on the ceiling. These may be suggestions for further optimization of the layout or permeability distribution, which could help to further reduce the flow losses.

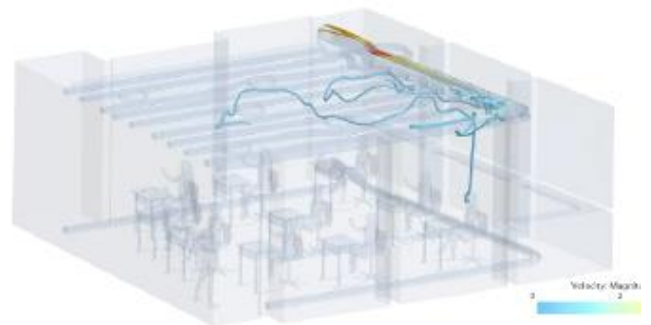


Fig. 17. Same as Fig. 16 but a different student. The virus protection effect is also apparent. Flow pattern is a bit more complex

Suppose we visualize all the particles in the room for a certain time. In that case, we get the following two pictures, where Fig. 18 shows the correct ventilation from bottom to top, Fig. 19 the wrong arrangement with ventilation from top to bottom, which counteracts thermal drift and therefore keeps many more particles in the whole room, although the same amount of air is exchanged and filtered equally efficiently.

One is tempted to consider the total number of particles as a measure of the quality of the process, but this leads to wrong conclusions because the particles collected overhead cannot contribute to the contagion and also cross-contamination is a superimposed local phenomenon.

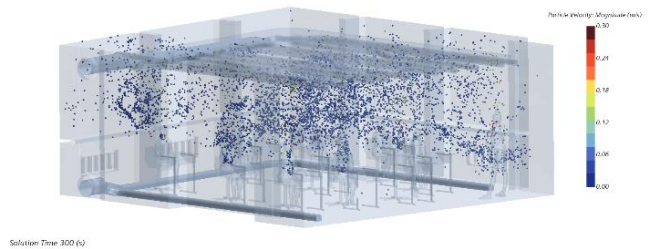


Fig. 18. Flow from floor the ceiling, all students exhaling particles. The lower part of the room stays clean, No cross contamination visible

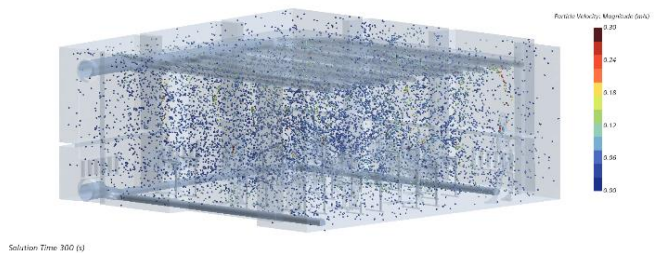


Fig. 19. Ventilation from ceiling to floor against the thermal body heat convection. Heavy cross contamination in the whole room results

It can be investigated by the numeric simulation, whether particles from student X – who may be infected – reach student Y, as was also done in [16, 22] for the contagion ratios in aircraft cabins. The calculation allows to run through this question for all students and to show only the "particle packets" that reach student Y, from each other student and the teacher. In the related overall picture Fig. 18, this "cross-contamination" phenomenon is hardly visible; the numbers in the considered control space are also small in relation to the total number in the space. Finally, Fig. 20 shows the total number of particles in the room during 300 seconds, wherein black represents the ventilation being switched off. In blue, the wrong direction of ventilation from top to bottom is assumed. In red, with the correct ventilation direction from the bottom to the top, a flattening effect quickly appears at low concentration. At the same time, the other two curves will continue to increase over time. For these 300 seconds, the high-performance computer already needs several days. The modeling allows to perform optimizations relatively quickly and agrees reasonably well with the experimental results below.

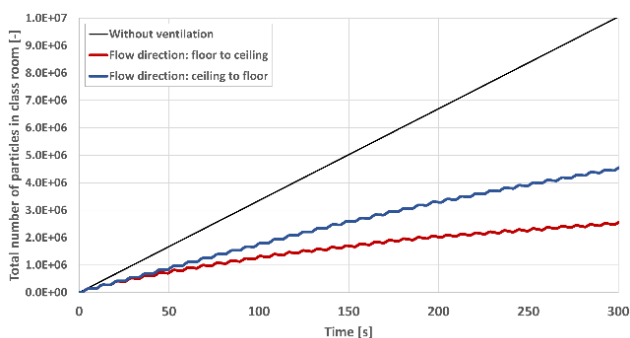


Fig. 20. Total particle number comparing 3 situations: without ventilation (black) ventilation from ceiling (blue) and from floor (red). Calculation for longer time further illustrate the flattening effect

9. Experimental analysis

The most crucial target of the experimental verification of the system functions was the scanning of the entire classroom with respect to nanoparticles released at one point, in order to quantitatively and repeatable verify the risk of infection or the reduction of this risk depending on the control parameters of the system. Since this is not possible in a crowded classroom, the thermal function of the bodies for vertical drift was replaced by adjustable heating plates of appropriate power and temperature (Fig. 21). Instead of a virus source, a nebulizer with a 3% NaCl-solution was placed, which emitted a very regular stream of droplets for 15 minutes (Fig. 22). The water evaporates within fractions of a second, leaving dry salt crystals. Thus, a salt particle cloud of a concentration of about 80,000 particles per cubic centimeter was generated at this location.



Fig. 21. Researcher installs the particle source at one desk, all other desks have particle counters and heated plates to simulate the students



Fig. 22. Nebulizer is used to form a spray of salt solution droplets, drying fast, forming a cloud of 30 nm particles, about 80'000 per cc

A particle counter was placed on each school desk to measure the particle concentration in the room. The elec-

tronic recording of the signals would provide a synchronous instantaneous picture of the distribution throughout the room in function of time. An optical counter from Sensirion was chosen as the sensor, which, however, only detects particles above 300 nm. The control with a diffusion charging device, which detects all particles above 10 nm, showed that although the Sensirion measurement only counts 1/25 of all particles, this factor remains largely constant so that the relations are detected accurately enough.

Figure 23 is the overall view and shows from these measurements the build-up of particle concentrations as the average value of all 10 sensors in the room over a period of 50 minutes after switching on the salt particle source. The blue curve reflects the case when the ventilation is switched off. The particle concentration in the whole room increases more or less linearly and would continue to increase, so after 2 hours, a concentration of about 4000 P/cc would be reached. In the case of the lower 3 curves, the system is in operation. A plateau is formed after a few minutes, which hardly changes even with a substantial increase in the total number of particles fed in (blue). In the case of green, the fan is running at target speed, in the case of red only at 60%, and in the case of the black curve, the heat sources have been switched on. After a running time of one hour, the entire room has only 10% of the particle concentration that would occur without the system; after two hours, it would be only about 5%, and so on.

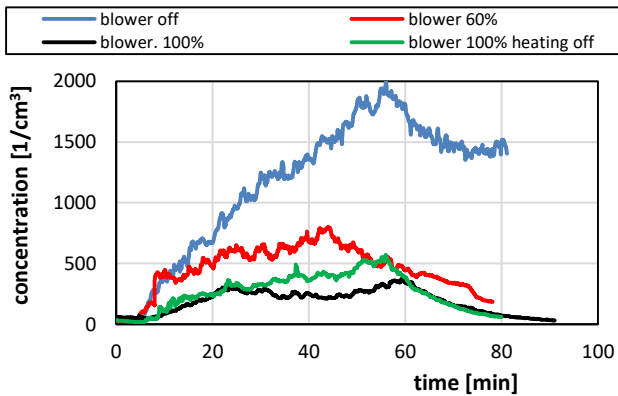


Fig. 23. Development of particle concentration after nebulizer start. Average of all desk counters. Without ventilation (blue), with 60% ventilation (red) with 100% ventilation (green); with body heat in addition (black)

Figure 24 is the single view of the lateral spreading, leading to an infection. Brown is the concentration at the source, repeatedly interrupted by refilling the nebulizer; the other colors show all other sensor locations in the whole room, including the two neighboring tables of the "infected", which are less than one meter away from the source. At first, the extraordinarily uniform distribution in the room is surprising, reaching a level of 2–300 P/cc after only 10 minutes, which hardly seems to change any further. In this case, the fan was running at nominal speed, and the heating plates were switched on, i.e., the case of the lowest curve of Fig. 23. The level of this set of curves is more than two

orders of magnitude below the level of the source. The risk of infection is thus reduced by a factor of > 100 even among the immediate neighbors of a potentially infected person.

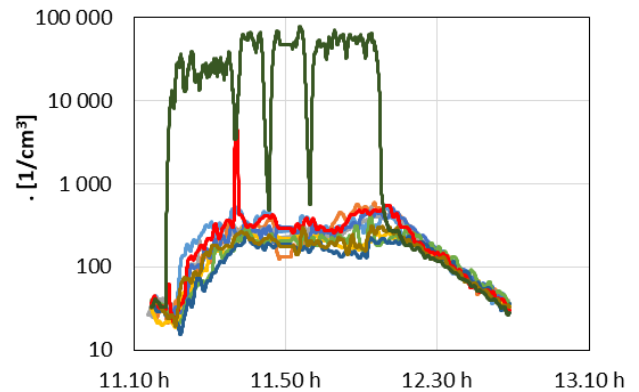


Fig. 24. Cross contamination defined by particle concentration of the source (80,000) compared to number at the desks (2–300), even at the neighbor desks. Distribution over the 10 desks is very uniform. Refill nebulizer four times

10. Conclusions

The use of vertical drift by body heat, combined with laminar ventilation from the floor to the ceiling, extraction of contaminated air from the ceiling, and nanofiltration of contaminated air, makes it possible to sustainably reduce the risk of infection by infectious agents such as corona viruses in closed rooms to a minimum of a few percent. This statement is valid even in case of high occupancy of the rooms, presence of several infected persons, and for a long time. At the same time, the fresh supply air is completely purified from carcinogenic ultrafine dust from traffic, and a CO₂-level is kept at the desired set point of 1000–1200 ppm. This method of leading the contaminated breathing air immediately after exhalation into the safe space "overhead" and removing it from there is not only applicable in buildings but in many other cases. In this way, the risk of virus spread among passengers of commercial airplanes could be virtually eliminated, where today individual ventilation from top to bottom explicitly contributes to a distribution of the viral load.

Acknowledgement

The authors would like to thank all those who contributed to the development of this method: the laboratories of the University of Applied Sciences of Northwestern Switzerland, the AMI-Institute of the University of Fribourg, the Rudolf Steiner Special School in Lenzburg, which made it possible to install the pilot plant in which no corona infections have been observed to date, the FOEN-UTF of the Swiss Federal Office for the Environment for the financial support, the advisory group from several federal offices as well as several private sponsors such as Dr. med. J. Schiltknecht, W. Johann, Dr. J. Mayer and the Swiss Lung Foundation.

Bibliography

- [1] Aoyagi Y, Takeuchi M, Yoshida K, Kurouchi M, Yasui N, Kamiko N et al. Inactivation of bacterial viruses in water using deep ultraviolet semiconductor light-emitting diode. *J Environ Eng.* 2011;137(12):1215-1218. [https://doi.org/10.1061/\(ASCE\)EE.1943-7870.0000442](https://doi.org/10.1061/(ASCE)EE.1943-7870.0000442)
- [2] Bischof OF. Recent developments in the measurement of low particulate emissions from mobile sources: a review of particle number legislations. *Emiss Control Sci Technol.* 2015;1:203-212. <https://doi.org/10.1007/s40825-015-0016-9>
- [3] Boger T, Glasson T, Rose D, Ingram-Ogunwumi R, Wu H. Next generation gasoline particulate filters for uncatylyzed applications and lowest particulate emissions. *SAE Int J Adv & Curr Prac in Mobility.* 2021;3(5):2452-2461. <https://doi.org/10.4271/2021-01-0584>
- [4] Brain JD and 200 scientists open letter addressed to WHO; Harvard Public School of Health, 2020.07.06.
- [5] Burtscher H, Lutz T, Mayer A. A new periodic technical inspection for particle emissions of vehicles. *Emiss Control Sci Technol.* 2019;5:279-287. <https://doi.org/10.1007/s40825-019-00128-z>
- [6] Collins KE, Cronin AA, Rueedi J, Pedley S, Joyce E, Humble PJ et al. Fate and transport of bacteriophage in UK aquifers as surrogates for pathogenic viruses. *Engineering Geology.* 2006;85:33-38. <https://doi.org/10.1016/j.enggeo.2005.09.025>
- [7] Curtius J, Granzin M, Schrod J. Testing mobile air purifiers in a school classroom. Reducing the airborne transmission risk for SARS-CoV-2. *Aerosol Sci Tech.* 2021;55(5):586-599. <https://doi.org/10.1080/02786826.2021.1877257>
- [8] Drewnick F et al. Abscheideeffizienz von Mund-Nasen-Schutz Masken. Max-Planck-Institut, Mainz 2020.04.30. https://www.mpic.de/4670174/filtermasken_zusammenfassung.pdf
- [9] Drossinos Y, Stilianakis NI. What aerosol physics tells us about airborne pathogen transmission, *Aerosol Sci Tech.* 2020;54(6):639-643. <https://doi.org/10.1080/02786826.2020.1751055>
- [10] Edwards DA, Ausiello D, Salzman J, Devlin T, Langer R, Beddingfield B et al. Exhaled aerosol increases with COVID-19 infection, age and obesity. *Biol Sci.* 2021;118(8):e2021830118. <https://doi.org/10.1073/pnas.202183011>
- [11] Fernely KP. Particle sizes of infectious aerosols; implications for infection control. *Lancet Respir Med.* 2020;8(9):914-924. [https://doi.org/10.1016/S2213-2600\(20\)30323-4](https://doi.org/10.1016/S2213-2600(20)30323-4)
- [12] Fuller CH, Brugge D. Ambient combustion ultrafine particles and health. Nova Science Publishers, Inc. New York. ISBN 978-1-53618-831-8.
- [13] Handbuch Verbrennungsmotor: Grundlagen, Komponenten, Systeme, Perspektiven. Springer Vieweg Verlag 8. ISBN 978-3-658-10901-1.
- [14] Hinds WC. *Aerosol Technology: Properties, Behavior, and Measurement of Airborne Particles.* John Wiley & Sons 1982, ISBN 0-471-08726-2.
- [15] Jing L. Charakterisierung der dieselmotorischen Partikel-emissionen. Dissertation der Universität Bern, 1997.
- [16] Khanh NC, Thai PQ, Quach HL, Thi NH, Dinh PC, Duong TN et al. Transmission of SARS-CoV 2 during long-haul flight. *Emerg Infect Dis.* 2020;26(11):2617-2624. <https://doi.org/10.3201/eid2611.203299>
- [17] Klompas M, Baker MA, Rhee C. Airborne transmission of SARS-CoV-2: theoretical considerations and available evidence. *JAMA.* 2020;324(5):441-442. <https://doi.org/10.1001/jama.2020.12458>
- [18] Lelieveld J, Helleis F, Borrmann S, Cheng Y, Drewnick F, Haug G et al. Model calculations of aerosol transmission and infection risk of COVID-19 in indoor environments. *Int J Env Res Pub He.* 2020;17(21):8114. <https://doi.org/10.3390/ijerph17218114>
- [19] Lexikon Motorentechnik; A. Mayer zu Partikelfiltern. Verlag Vieweg, ISBN 3-528-03903-5.
- [20] Lieber C, Melekidis S, Koch R, Bauer HJ. Insights into the evaporation characteristics of saliva droplets and aerosols: levitation experiments and numerical modeling. *J Aerosol Sci.* 2021;154:105760. <https://doi.org/10.1016/j.jaerosci.2021.105760>
- [21] Lindsley WG, Derk RC, Coyle JP, Martin SB, Mead KR, Blachere FM et al. Efficacy of portable air cleaners and masking for reducing indoor exposure to simulated exhaled SARS-CoV-2 aerosols. *MMWR Morb Mortal Wkly Rep.* 2021; 70(27):972-976. <https://doi.org/10.15585/mmwr.mm7027e1>
- [22] Liu J, Huang J, Xiang D. Large SARS-CoV-2 outbreak caused by asymptomatic traveler, China. *Emerg Infect Dis.* 2020;26(9):2260-2263. <https://doi.org/10.3201/eid2609.201798>
- [23] Marr LC, Tang JW, Mullekom J, Lakdawala SS. Mechanistic insights into the effect of humidity on airborne influenza virus survival, transmission and incidence. *J R Soc Interface.* 2019; 16(150):201850298. <https://doi.org/10.1098/rsif.2018.0298>
- [24] Miller JH. Experiments in molecular genetics. *The Quarterly Review of Biology.* 1974;49(2). <https://doi.org/10.1086/408025>
- [25] Morawska L, Cao J. Airborne transmission of SARS-CoV-2: The world should face the reality. *Environ Int.* 2020;139: 105730. <https://doi.org/10.1016/j.envint.2020.105730>
- [26] NanoCleanAir. www.nanocleanair.ch
- [27] Riediker M, Monn C. Simulation of SARS-CoV-2 aerosol emissions in the infected population and resulting airborne exposures in different indoor scenarios; Aerosol Drivers, Impacts and Mitigation. 2021;21(2):20. <https://doi.org/10.4209/aaqr.2020.08.0531>
- [28] Rüggeberg T, Milosevic A, Specht P, Mayer A, Frey J, Petri-Fink A et al. A versatile filter test system to assess removal efficiency for viruses in aerosols. *Aerosol Air Qual Res.* 2021;21:210224. <https://doi.org/10.4209/aaqr.210224>
- [29] Schmid S, Seiler C, Gerecke AC, Hächler H, Hilbi H, Frey J et al. Studying the fate of non-volatile organic compounds in a commercial plasma air purifier. *J Hazard Mater.* 2013;256-257:76-83. <https://doi.org/10.1016/j.jhazmat.2013.04.021>
- [30] Silverman DT, Samanic CM, Lubin JH, Blair AE, Stewart PA, Vermeulen R et al. The diesel exhaust in miners study: a nested case-control study of lung cancer and diesel exhaust. *J Natl Cancer Inst.* 2012;104(11):855-868. <https://doi.org/10.1093/jnci/djs034>
- [31] TSI Incorporated. www.tsi.com
- [32] van Doremalen N, Bushmaker T, Morris DH, Holbrook MG, Gamble A, Williamson BN et al. Aerosol and surface stability of SARS-CoV-2. *N Engl J Med.* 2020;382:1564-1567. <https://doi.org/10.1056/NEJMc2004973>
- [33] VERT-Filter List www.vert-certification.eu
- [34] Vohra K, Vodonos A, Schwartz J, Marais EA, Sulprizio MP, Mickley LJ. Global mortality from outdoor fine particle pollution generated by fossil fuel combustion: results from GEOS-Chem. *Environ Res.* 2021;195:110754. <https://doi.org/10.1016/j.envres.2021.110754>

- [35] World Health Organization. <https://www.who.int/>
[36] Zhang R, Li Y, Zhang AL, Molina MJ. Identifying airborne transmission as the dominant route for the spread of COVID-

19. Earth, Atmospheric, and Planetary Sciences. 2020; 117(26):14857-14863.
<https://doi.org/10.1073/pnas.200963711>

Prof. em. Dr. Jan Czerwiński – Nano, NanoCleanAir GmbH, Switzerland.
e-mail: cjcons19@gmail.com



Dipl. Ing. Dr. med. h.c. Andreas Mayer – CEO NanoCleanAir GmbH, Switzerland.
e-mail: a.mayer@nanocleanair.ch



Dipl. Ing. ETH. Dr. Jörg Mayer – Nano, NanoCleanAir GmbH, Switzerland.
e-mail: j.mayer@nanocleanair.ch



Prof. em. Dr. Heinz Burtscher – Institute for Sensors and Electronics, Fachhochschule Nordwestschweiz, Windisch, Switzerland.
e-mail: h.burtscher@nanocleanair.ch



Dipl. Ing. ETH Thomas Lutz – Nano, NanoCleanAir GmbH, Switzerland.
e-mail: t.lutz@nanocleanair.ch



MSc. BBA Rainer Mayer – Nano, NanoCleanAir GmbH, Switzerland.
e-mail: r.mayer@nanocleanair.ch



Prof. Dr. Barbara Rothen-Rutishauser – Adolphe Merkle Institute, University Fribourg, Switzerland.
e-mail: barbara.rothen@unifr.ch



Prof. em. Dr. Joachim Frey – Vetsuisse Faculty, University Berne, Switzerland.
e-mail: joachim.frey@unibe.ch



Dr. sc. techn., Dipl. Ing. ETH Christian Lämmle – Combustion Flow, Combustion Flow Solutions GmbH, Switzerland.
e-mail: laemml@combustion-flow-solutions.ch



BSc Energy and Environmental Technology (FHNW), Tobias Rüggeberg – Institute for Sensors and Electronics, Fachhochschule Nordwestschweiz, Windisch, Switzerland.
e-mail: tobias.rueggeberg@fhnw.ch



Dipl. Ing. Patrick Specht – Institute for Sensors and Electronics, Fachhochschule Nordwestschweiz, Windisch, Switzerland.
e-mail: patrick.specht@fhnw.ch

